Water-Insoluble Organics Dominate Brown Carbon in Wintertime Urban Aerosol of China

Huang, Ru Jin; Yang, Lu; Shen, Jincan; Yuan, Wei; Gong, Yuquan; Guo, Jie; Cao, Wenjuan; Duan, Jing; Ni, Haiyan; Zhu, Chongshu

Published in:
Environmental Science and Technology

DOI:
10.1021/acs.est.0c01149

Environmental Science & Technology

pubs.acs.org/est Article

Water-Insoluble Organics Dominate Brown Carbon in Wintertime Urban Aerosol of China: Chemical Characteristics and Optical Properties

Ru-Jin Huang,* Lu Yang, Jincan Shen,* Wei Yuan, Yuquan Gong, Jie Guo, Wenjuan Cao, Jing Duan, Haiyan Ni, Chongshu Zhu, Wenting Dai, Yongjie Li, Yang Chen, Qi Chen, Yunfei Wu, Renjian Zhang, Ulrike Dusek, Colin O'Dowd, and Thorsten Hoffmann

Cite This: *Environ. Sci. Technol.* 2020, 54, 7836−7847

ABSTRACT: The chromophores responsible for light absorption in atmospheric brown carbon (BrC) are not well characterized, which hinders our understanding of BrC chemistry, the links with optical properties, and accurate model representations of BrC to global climate and atmospheric oxidative capacity. In this study, the light absorption properties and chromophore composition of three BrC fractions of different polarities were characterized for urban aerosol collected in Xi'an and Beijing in winter 2013−2014. These three BrC fractions show large differences in light absorption and chromophore composition, but the chromophores responsible for light absorption are similar in Xi'an and Beijing. Water-insoluble BrC (WI-BrC) fraction dominates the total BrC absorption at 365 nm in both Xi'an (51 ± 5%) and Beijing (62 ± 13%), followed by a humic-like fraction (HULIS-BrC) and high-polarity water-soluble BrC. The major chromophores identified in HULIS-BrC are nitrophenols and carbonyl oxygenated polycyclic aromatic hydrocarbons (OPAHs) with 2−3 aromatic rings (in total 18 species), accounting for 10% and 14% of the light absorption of HULIS-BrC at 365 nm in Xi'an and Beijing, respectively. In comparison, the major chromophores identified in WI-BrC are PAHs and OPAHs with 4−6 aromatic rings (in total 16 species), contributing 6% and 8% of the light absorption of WI-BrC at 365 nm in Xi'an and Beijing, respectively.

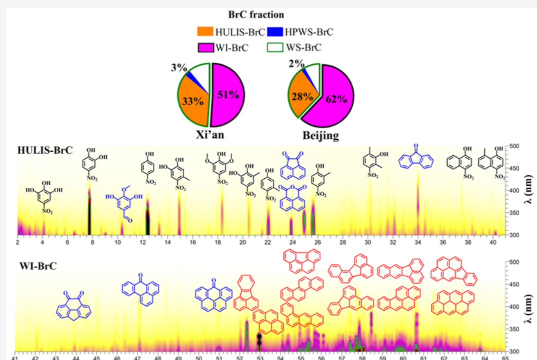

■ INTRODUCTION

Light-absorbing organic carbon, also known as brown carbon (BrC), is ubiquitous in the atmosphere.[1−8] Growing evidence have shown that the light absorption of solar radiation by BrC can affect the atmospheric photochemistry through decreasing the photolysis frequencies and influence the regional and global climate by changing the radiative balance.[9−14] This has motivated many laboratory and field studies focusing on the optical properties, sources, and radiative forcing of BrC.[15−26] BrC can be emitted directly from incomplete combustion of biomass and coal[27−30] or formed through multiphase reactions in the atmosphere, referred to as "secondary BrC".[31−33] Atmospheric aging processes, on the other hand, lead to a dynamic transformation of BrC in its physicochemical properties, which can either enhance or reduce the light absorption of BrC.[34−36] The complexity in sources and dynamic variation in chemical composition make it difficult to characterize the molecular composition of BrC and its link to light absorption properties.

Field measurements have identified some BrC chromophores, including nitrophenols and polycyclic aromatic hydrocarbons (PAHs). For example, Zhang et al.[37] identified eight nitrophenol compounds in aerosol extracts in the Los Angeles Basin, which contributed to ∼4% of water-soluble BrC light absorption at 365 nm. Mohr et al.[38] quantified five nitrophenols in ambient aerosol in Detling, United Kingdom, which accounted for ∼4% of BrC light absorption at 370 nm. In cloudwater samples collected at Mount Tai in China, which was heavily affected by biomass burning, Desyaterik et al.[39] identified 16 major light-absorbing compounds (mainly nitrophenols and aromatic carbonyl compounds), which contributed to ∼50% of BrC light absorption between 300 and 400 nm. Our previous studies found that 18 PAHs and carbonyl oxygenated PAHs (OPAHs) accounted for on average ∼1.7% of the overall absorption of methanol-soluble BrC in urban Xi'an, which was about 5 times higher than their mass fraction in total organic carbon.[40] These studies suggest

Received: February 24, 2020
Revised: May 25, 2020
Accepted: June 1, 2020
Published: June 1, 2020

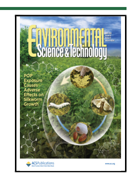

that even a small fraction of highly light-absorbing organics may have a significant effect on the optical properties of BrC. However, the identification of BrC chromophores is a very challenging analytical task due to the low concentrations of light-absorbing molecules in complex organic mixtures.[41]

BrC consists of both water-soluble and water-insoluble components and is often categorized into water-soluble and methanol-soluble/water-insoluble BrC to describe the optical properties.[42−44] The water-insoluble fraction of BrC has a greater absorption per unit of mass than the water-soluble fraction,[37,44] due to the difference in chromophores. However, neither the water-soluble nor the water-insoluble BrC components have been well characterized on a molecular level so far, hindering a better understanding of the link between BrC chromophores and light absorption properties. In this study, BrC aerosol from wintertime Beijing and Xi'an are separated into three subfractions on the basis of its polarity and water solubility. The abundance and light absorption properties of these BrC subfractions are analyzed. Moreover, the BrC chromophores in different fractions are characterized using a high-performance liquid chromatograph (HPLC) equipped with a photodiode array (PDA) for UV−vis absorption measurements and a high-resolution Orbitrap mass spectrometer (HRMS). The contributions of different BrC chromophores to the light absorption of different BrC fractions are also investigated.

■ EXPERIMENTAL SECTION

Sample Collection. Daily $PM_{2.5}$ samples (24 h integrated) were collected from December 19, 2013, to January 6, 2014, in Xi'an and from January 10 to 25, 2014, in Beijing. The Xi'an samples were collected on the rooftop of a building (∼10 m above the ground level) in downtown (34.23°N, 108.88°E), and Beijing samples were collected on the rooftop (∼20 m above the ground level) in downtown (40.00°N, 116.38°E). These samples were collected on prebaked (780 °C for 3 h) quartz-fiber filters (20.3 × 25.4 cm, Whatman, QM-A) using a high-volume sampler (Tisch, Cleveland, OH) at a flow rate of 1.05 m^3 min^{-1}. After sampling, the filter samples were sealed in aluminum foil bags and stored at −20 °C in the dark until analysis.

Extraction of BrC Fraction. A portion of the filter (1.5−4 cm^2) was used to extract BrC into different fractions, similar to previous studies.[45−48] The water-soluble fraction was extracted twice with 5 mL of Milli-Q water under ultrasonication for 30 min and was filtered through a syringe filter (Puradisc13 PVDF, 0.45 μm, Whatman). Afterward, the residual filter was dried and the water-insoluble fraction was further extracted twice with 5 mL of methanol (HPLC grade) under ultrasonication for 30 min. The methanol extracts were then filtered through a PVDF syringe filter for further analysis. The change in color on the filters to colorless suggests that the majority of light-absorbing compounds were extracted. The water-soluble fraction was further separated into two fractions following a solid-phase extraction (SPE) method similar to that described by Varga et al.[49] and Lin et al.[50] Briefly, the water-soluble extracts were acidified to pH 2 using HCl (2.4 M) and then passed through an SPE cartridge (Oasis HLB, 3 cc, 60 mg; Waters). Those not retained in the SPE cartridge are high-polarity water-soluble organics, while those retained in the SPE cartridge are considered as humic-like substances (HULIS). The HULIS subfraction was eluted with 2 mL of methanol containing 2% (wt) ammonia, evaporated to dryness under a gentle stream of nitrogen, and redissolved into a known amount of ultrapure water for subsequent analysis. Detailed analysis steps for different OC and BrC fractions are shown in Figure S1. In addition, one combined filter sample (0.126−1.05 cm^2 of the filter taken from each sample to ensure similar OC contents from each filter) in both Xi'an and Beijing was extracted with the same procedure (20 mL solvent for extraction) described above and the extracts of the corresponding high-polarity water-soluble, HULIS, and water-insoluble fractions were concentrated to 200 μL for subsequent HPLC-PDA-HRMS analysis.

Analysis of Carbonaceous Components and Ions. The concentrations of OC and EC were measured by a thermal/optical carbon analyzer (DRI Model 2001, Desert Research Institute) following the IMPROVE-A temperature protocol.[51] The carbon concentration in HULIS and water-soluble organic carbon (WSOC) was determined by a Shimadzu 5000 TOC/N analyzer.[52] The difference between OC and WSOC is water-insoluble organic carbon (WISOC), while the difference between WSOC and HULIS-C is high-polarity WSOC (HP-WSOC). Inorganic ions, including NO_3^-, SO_4^{2-}, Cl^-, Na^+, K^+, Mg^{2+}, Ca^{2+}, and NH_4^+, were analyzed using ion chromatography (DX-600, Dionex), and a detailed analytical procedure is described in the Supporting Information.

Light Absorption Spectra Measurement. Light absorption spectra of extracts of the three fractions were measured with a UV−vis spectrophotometer (300−700 nm) coupled with a liquid waveguide capillary cell (LWCC-3100, World Precision Instrument), following the method established in Hecobian et al. (2010).[16] The absorption coefficient of organics in extract can be calculated as

$$\mathrm{Abs}_\lambda = (A_\lambda - A_{700})\frac{V_l}{V_a \times l}\ln 10 \tag{1}$$

where Abs_λ (Mm^{-1}) represents the absorption coefficient of the HULIS BrC fraction (HULIS-BrC) for the HULIS extract, the high-polarity water-soluble BrC fraction (HPWS-BrC) for HP-WSOC, the water-soluble BrC fraction (WS-BrC) for WSOC, and the water-insoluble BrC fraction (WI-BrC) for WISOC at a wavelength of λ. A_λ is the absorbance recorded, V_l (in mL) is the volume of extracts, V_a (in m^3) is the volume of the air sampled through the filter punch, and l is the optical path (0.94 m). The sum of WS-BrC and WI-BrC is the total BrC (Tot-BrC). The mass absorption efficiency (MAE, m^2 g C^{-1}) of the BrC fractions in the extracts at wavelength of λ can be described as[44]

$$\mathrm{MAE}_\lambda = \frac{\mathrm{Abs}_\lambda}{C} \tag{2}$$

where C (μg C m^{-3}) represents the atmospheric concentration of HULIS-C, HP-WSOC, and WISOC for HULIS-BrC, HPWS-BrC, and WI-BrC, respectively. Note that since it is impossible that all of the WI-BrC compounds were extracted into methanol, the light absorption of WI-BrC reported in this study is likely the lower limit. However, the underestimate is likely insignificant because of the high extraction efficiency (88 ± 5%) of OC by methanol. The wavelength dependence of BrC light absorption (absorption Angström exponent, AAE) is calculated by fitting the linear regression of log Abs_λ with log λ in the wavelength range of 300−500 nm.[44]

HPLC-PDA-HRMS Analysis and Data Processing. The extracts of HP-WSOC, HULIS, and WISOC fractions were

https://dx.doi.org/10.1021/acs.est.0c01149
Environ. Sci. Technol. 2020, 54, 7836−7847

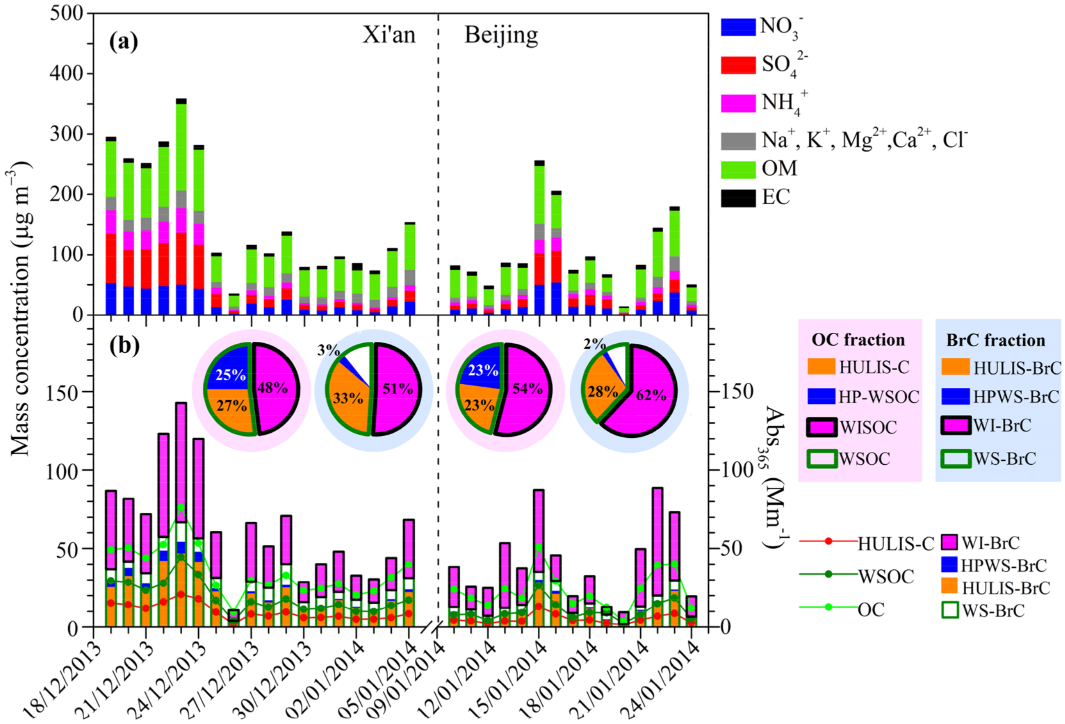

Figure 1. Time series of (a) the main $PM_{2.5}$ species (OM = 1.5 × OC) and (b) the light absorption coefficients of BrC fractions at 365 nm (Abs_{365}) and the concentrations of HULIS-C, WSOC, and OC. The pie charts in panel (b) represent the mean percentages of individual OC and BrC fractions. The white slices in the pie charts of BrC fractions represent the light absorption caused by intermolecular interactions or complex formation between HULIS and HP-WSOC.

Table 1. Summary of Organic Carbon Components and BrC Fractions in the Aerosol Samples of Xi'an and Beijing during Winter of 2013/2014

component	Xi'an (n = 18) range	mean	std[a]	Beijing (n = 15) range	mean	std
HULIS-C (μg C m^{-3})	2.4−26.3	12.4	6.5	2.0−16.5	6.4	3.8
HP-WSOC (μg C m^{-3})	2.5−29.7	11.6	6.5	1.0−16.9	6.4	4.2
WISOC (μg C m^{-3})	7.5−39.9	20.8	7.9	1.6−30.7	16.3	8.9
OC (μg C m^{-3})	12.4−95.9	44.8	20.1	4.6−64.0	29.1	15.7
$Abs_{365,HULIS\text{-}BrC}$ (Mm^{-1})	2.8−47.0	22.6	11.9	1.4−27.4	11.5	7.5
$Abs_{365,HPWS\text{-}BrC}$ (Mm^{-1})	0.2−7.1	2.3	2.3	0.1−2.6	0.5	0.6
$Abs_{365,WS\text{-}BrC}$ (Mm^{-1})	4.1−66.8	31.5	16.4	1.9−29.6	15.0	9.5
$Abs_{365,WI\text{-}BrC}$ (Mm^{-1})	6.7−75.9	33.9	16.4	4.9−68.5	26.1	18.4
$Abs_{365,total\ BrC}$ (Mm^{-1})	10.8−142.7	65.4	35.4	9.5−87.2	42.1	21.3
HULIS-C/WSOC	0.44−0.58	0.52	0.03	0.41−0.68	0.51	0.09
HULIS-C/OC	0.19−0.36	0.27	0.04	0.17−0.29	0.23	0.04
WISOC/OC	0.37−0.57	0.48	0.07	0.36−0.68	0.54	0.11
HULIS-BrC/WS-BrC[b]	0.63−0.78	0.71	0.04	0.69−0.81	0.75	0.06
HULIS-BrC/Tot-BrC[b]	0.26−0.40	0.35	0.04	0.15−0.47	0.28	0.09
WI-BrC/Tot-BrC[b]	0.20−0.63	0.51	0.05	0.36−0.80	0.62	0.13

[a]std denotes the standard deviation. [b]The ratio of light absorption coefficients at 365 nm.

analyzed by a HPLC-PDA-HRMS system consisting of a Dionex UltiMate 3000 HPLC system (Thermo Electron, Inc.) and a high-resolution Q Exactive Plus hybrid quadrupole-Orbitrap mass spectrometer (Thermo Electron, Inc.). The separation was conducted on a Thermo Accucore RP-MS column (2.1 × 100 mm, 2.6 μm particle size). A binary gradient elution was applied, with mobile phase A being 0.1% formic acid in water and mobile phase B being 0.1% formic acid in methanol at a flow rate of 0.3 mL min^{-1}. The gradient elution was set as follows: the concentration of B was held at 15% at the beginning and then linearly increased to 30% from 0 to 20 min, linearly increased to 90% from 20 to 60 min, held at 90% from 60 to 70 min, and then decreased to 15% from 70 to 72 min and held there for 80 min. The UV−vis absorption spectra were obtained using the PDA detector at a wavelength range of 190−700 nm. The absorption spectrum of the bulk solution was also measured by the PDA detector without HPLC separation. The Q Exactive Plus hybrid quadrupole-Orbitrap mass spectrometer was equipped with an electrospray ionization (ESI) source. It was operated with 40 units of sheath gas flow, 8 units of auxiliary gas flow, 350 °C capillary temperature, and −3.2 kV spray voltage in the negative mode

https://dx.doi.org/10.1021/acs.est.0c01149
Environ. Sci. Technol. 2020, 54, 7836−7847

(ESI (−)) and 3.5 kV spray voltage in the positive mode (ESI (+)). Mass spectra of different BrC fractions of combined samples in both Xi'an and Beijing were acquired in both ESI (−) and ESI (+) modes in the mass range between m/z 100 and 800 with a resolving power of 70000 at m/z 200. Authentic standards of 13 nitrophenols and 15 PAHs (Table S1) were analyzed with the same approach. Data were processed with the Xcalibur 4.0 software (Thermo Scientific). The elemental composition of individual chromatographic peaks was assigned with the molecular formula calculator in Xcalibur 4.0 software using a mass tolerance of ±3 ppm. The maximum numbers of atoms for the formula calculator were set as follows: 30 ^{12}C, 60 ^{1}H, 15 ^{16}O, 3 ^{14}N, 1 ^{32}S and 1 ^{23}Na. Formulas with a close match between theoretical ion mass and observed ion mass were selected. To eliminate the chemically unreasonable formulas, the identified formulas were constrained by setting $0.3 \leq H/C \leq 3.0$, $0.0 \leq O/C \leq 3.0$, $0.0 \leq N/C \leq 0.5$, $0.0 \leq S/C \leq 0.2$.[53] Further, As suggested by Lin et al.,[54] only those with $DBE/C \geq 0.5$ were considered as candidates of BrC chromophores. For a chemical formula of $C_cH_hO_oN_nS_sNa_x$, the double-bond equivalent (DBE; that is, the number of rings plus double bonds to carbon) was calculated as $DBE = (2C + 2 - H + N)/2$, and the aromaticity index (AI) was calculated as $AI = (1 + C - O - S - 0.5H)/(C - O - N - S)$.[55] Calculated neutral molecular formulas that did not fit the nitrogen rule or exhibited a noninteger or negative DBE were excluded. All of the results reported were corrected for blanks.

RESULTS AND DISCUSSION

Chemical and BrC Fraction. Figure 1a shows the temporal variations of $PM_{2.5}$ chemical components in Xi'an and Beijing. Organic matter (OM) is the major component of urban $PM_{2.5}$ species, accounting for 46 ± 9% and 45 ± 8% of the quantified $PM_{2.5}$ species in Xi'an and Beijing, respectively. The variations of different OC and BrC fractions are shown in Figure 1b, and the results are summarized in Table 1. Among the separated OC fractions, WISOC was the most abundant fraction with average concentrations of 20.8 ± 7.9 and 16.3 ± 8.9 μg C m^{-3}, accounting for 48 ± 7% and 54 ± 11% of OC in Xi'an and Beijing, respectively. HULIS-C contributed 27 ± 4% (12.4 ± 6.5 μg C m^{-3}) and 23 ± 4% (6.4 ± 3.8 μg C m^{-3}) to OC in Xi'an and Beijing, respectively, while the corresponding contributions from HP-WSOC, the most polar fraction, were 25 ± 3% (11.6 ± 6.5 μg C m^{-3}) and 22 ± 9% (6.4 ± 4.2 μg C m^{-3}). It is noted that the concentration of HULIS-C in Xi'an was about twice that in Beijing. However, the fractional contributions of HULIS-C in WSOC were rather similar in Xi'an and Beijing (~50%).

Consistent with the dominance of WISOC in OC, WI-BrC was also the most abundant fraction of BrC in both Xi'an and Beijing. The average Abs_{365} of WI-BrC was 33.9 ± 16.4 Mm^{-1} in Xi'an and 26.1 ± 18.4 Mm^{-1} in Beijing, which was higher than that of HULIS-BrC (22.6 ± 11.9 Mm^{-1} in Xi'an and 11.5 ± 7.5 Mm^{-1} in Beijing) and HPWS-BrC (2.3 ± 2.3 Mm^{-1} in Xi'an and 0.5 ± 0.6 Mm^{-1} in Beijing), highlighting the significance of WI-BrC in aerosol light absorption in urban areas in winter. It is noted that the contribution of WI-BrC to Tot-BrC was higher in Beijing (62 ± 13%) than in Xi'an (51 ± 5%) ($p < 0.01$), although the fractional contributions of WISOC in OC were similar in Beijing and Xi'an ($p = 0.06$). HULIS-BrC is also an important BrC fraction, with average Abs_{365} value of 22.6 ± 11.9 and 11.5 ± 7.5 Mm^{-1} in Xi'an and Beijing, respectively. The average Abs_{365} value of HULIS-BrC was about 10 times higher than that of HPWS-BrC in both Xi'an and Beijing, although the fractional contributions of HULIS-C and HP-WSOC in OC were similar in both Xi'an and Beijing, suggesting a higher absorption efficiency of HULIS-BrC in comparison to HPWS-BrC. It should be noted that the sum of Abs_{365} of HULIS-BrC and HPWS-BrC was ~20% lower (22% lower in Xi'an and 24% lower in Beijing) than that of WS-BrC, consistent with the results in Chen et al.[45] Given that the recovery of the SPE procedure is ~100%,[49,50] such a difference is likely due to intermolecular interactions between aromatic compounds with multiple hydroxyl, aldehyde, or ketone groups and the formation of complexes between aromatic compounds with multiple hydroxyl groups (mainly in HULIS) and transition metals (mainly in HP-WSOC), which leads to an enhancement in light absorption.[56,57]

Optical Properties of BrC Fraction. The light absorption spectra (300−500 nm) of different BrC fractions in Xi'an and Beijing are shown in Figure S2. They all show rapidly increasing absorption toward shorter wavelengths. It can be seen from the figure that the sum of light absorption of HULIS-BrC and HPWS-BrC was lower than that of WS-BrC in the wavelength range of 300−500 nm in both Xi'an and Beijing (on average, 23% and 26% lower in Xi'an and Beijing, respectively), which may be attributed to intermolecular interactions and/or formation of complexes between HULIS and HP-WSOC fractions, as discussed above. Figure 2 shows

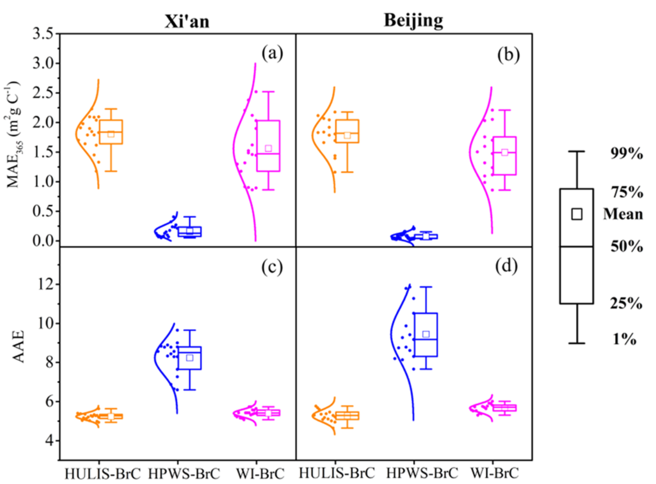

Figure 2. MAE_{365} and AAE of fractionated BrC in Xi'an (a, c) and Beijing (b, d).

the statistical results of AAE for different BrC fractions. The average AAE values of HULIS-BrC are similar in Xi'an (5.2 ± 0.2) and Beijing (5.3 ± 1.3). The AAE of HPWS-BrC is much higher than that of HULIS-BrC in both Xi'an and Beijing with average values of 8.2 ± 1.0 and 9.4 ± 2.6, respectively, which could be associated with the lower conjugated degree and molecular weight of chromophores in HP-WSOC in comparison to HULIS. However, the AAE values of WI-BrC are similar to those of HULIS-BrC in both Xi'an (5.4 ± 0.2) and Beijing (5.7 ± 0.2).

The MAE of different BrC fractions depends mainly on the chemical structure of the chromophores (e.g., unsaturation degree, oxidation state, and molecular weight) and the ratio of chromophore species to non-light-absorbing organics. Among

https://dx.doi.org/10.1021/acs.est.0c01149
Environ. Sci. Technol. 2020, 54, 7836−7847

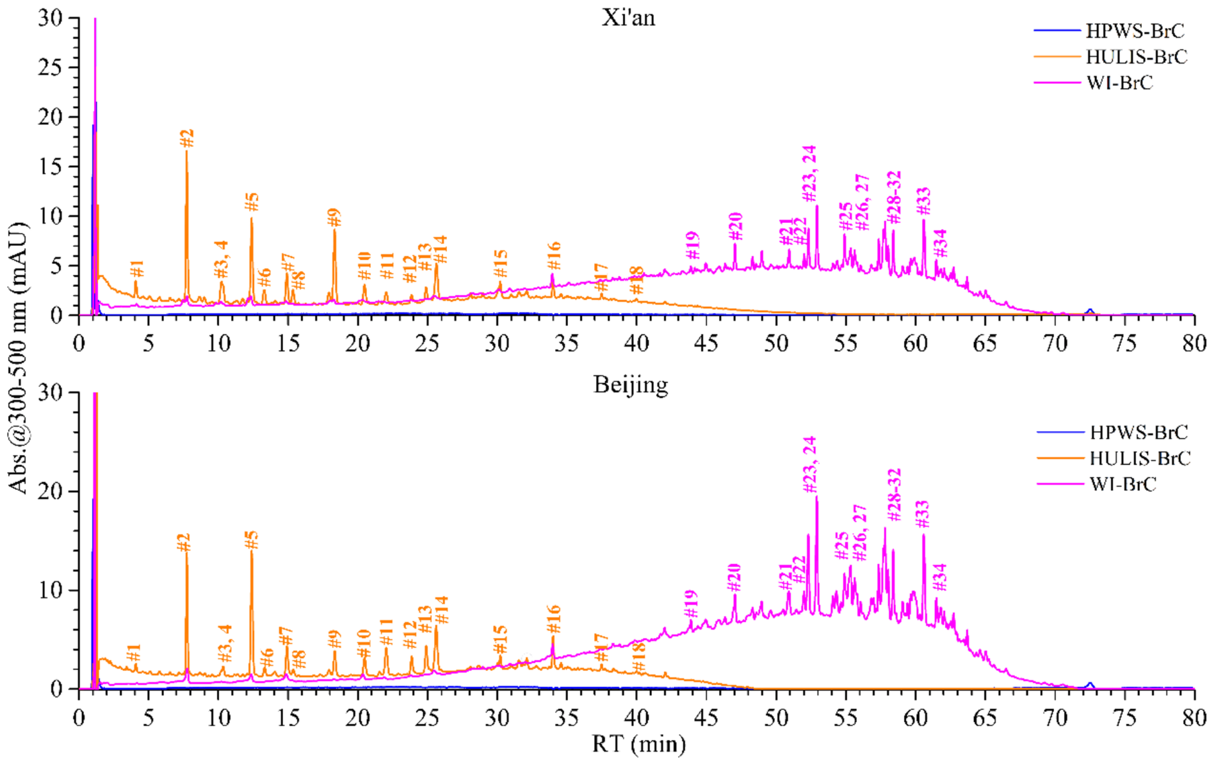

Figure 3. HPLC-PDA absorption chromatograms of BrC fractions integrated over the wavelength range of 300−500 nm and the number of major identified BrC chromophores in HULIS-BrC (#1−18) and WI-BrC (#19−34). Note that the aerosol sampling volumes are the same for the three BrC fractions.

the BrC fractions, the MAE_{365} of HULIS-BrC is the highest, with average of 1.8 ± 0.3 m^2 g C^{-1} in Xi'an and 1.8 ± 0.4 m^2 g C^{-1} in Beijing, which is relatively higher in comparison to that (1.84 ± 0.77 m^2 g^{-1}, equal to 0.97 ± 0.40 m^2 g^{-1} C using an OM/OC ratio of 1.9) observed in an urban site of Hong Kong.[21] The MAE_{365} of HPWS-BrC, however, is about 1 order of magnitude lower than that of HULIS-BrC, most likely because HP-WSOC mainly consists of low-molecular-weight organic acids, sugars, and highly oxidized organic matter, which exhibit relatively weak light absorption in comparison to the aromatic conjugated systems and macromolecules in HULIS-BrC.[45] The MAE_{365} of WI-BrC is also slightly lower than that of HULIS-BrC in both Xi'an and Beijing, with averages of 1.5 ± 0.5 m^2 g C^{-1} in Xi'an and 1.5 ± 0.4 m^2 g C^{-1} in Beijing, which is about 5 times higher than that observed (0.2−0.4 m^2 gC^{-1}) in Nagoya, Japan.[45] It should be noted that the average MAE_{365} values are very close between Xi'an and Beijing for both HULIS-BrC and WI-BrC, indicating the similarity of BrC composition between Xi'an and Beijing. To ascertain this preliminary conclusion, we further investigated the chemical composition of chromophores in different BrC fractions, as discussed below.

Chemical Composition of BrC Chromophores. Figure 3 shows the HPLC-PDA chromatograms of different BrC fractions in Xi'an and Beijing. They are integrated absorptions from 300 to 500 nm and show different profiles, with major fractions being eluted between 0 and 2 min for HPWS-BrC, between 3 and 40 min for HULIS-BrC, and between 40 and 70 min for WI-BrC. The difference in retention behavior of these three BrC fractions can be explained by their different polarities and/or hydrophilicities. The poor retention of HPWS-BrC chromophores in the Accucore RP-MS column could be attributed to their relatively polar and/or hydrophilic properties relative to the stationary phase. In comparison to HPWS-BrC, HULIS-BrC is less polar and a majority of the chromophores are well separated between 3 and 40 min, while WI-BrC is the least polar and hydrophilic fraction and thus its chromophores are eluted much later (40−70 min). In addition to the different retention behavior, these three BrC fractions also show differences in the chromatographic baseline. The baseline absorption spectra of HULIS-BrC is much higher than that of HPWS-BrC in a retention time between 3 and 40 min and are similar to those of the bulk solution with no obvious absorption peak in the wavelength range of 300−500 nm. This indicates the coelution of a large number of light-absorbing species with weak light absorption and/or low concentration.[39] The PDA absorption chromatograms of WI-BrC, however, exhibit a broad "bump" at a retention time of 40−65 min, which is similar to those observed for biomass burning and photo-oxidation of toluene secondary organic aerosol, suggesting the presence of an unresolved complex mixture consisting of numerous light-absorbing species.[58,59] As it is difficult to assign particular chromophores responsible for the enhanced baseline and broad "bump", we focus on the identification of HULIS-BrC and WI-BrC chromophores that have resolved peaks in the HPLC-PDA absorption chromatograms.

The elemental formulas of those ions in the mass spectrum with retention times matching with the PDA absorption chromatographic peaks were assigned using the procedure described in the Experimental Section, and only those with high DBE values of >4 were considered as candidates of BrC chromophores. Furthermore, unambiguous or tentative structures of BrC chromophores were assigned by comparing with authentic standard compounds or reference UV−vis

https://dx.doi.org/10.1021/acs.est.0c01149
Environ. Sci. Technol. 2020, 54, 7836−7847

Table 2. Retention Times (RTs), UV−Vis Spectra, Elemental Formulas and Assigned Structures of Identified BrC Chromophores[a]

#	RT (min)	UV-Vis Spectrum	Formula	m/z & ion mech.[1]	Unambiguous/Tentative structure	Ref. Sample	#	RT (min)	UV-Vis Spectrum	Formula	m/z & ion mech.	Unambiguous/Tentative structure	Ref. Sample
1	4.08		$C_6H_5NO_5$	170.00977 [M-H]$^-$	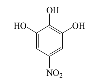 nitropyrogallol	66 BBOA	6	13.32		$C_7H_5NO_5$	182.00961 [M-H]$^-$	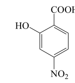 4-nitrosalicylic acid	66 BBOA
2	7.78		$C_6H_5NO_4$	154.01446 [M-H]$^-$	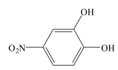 4-nitrocatechol	S[2]	7	14.92		$C_7H_7NO_4$	168.03014 [M-H]$^-$	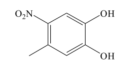 4-methyl-5-nitrocatechol	S
3	10.16		$C_7H_7NO_5$	184.02499 [M-H]$^-$	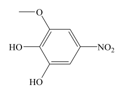 3-methoxy-4-nitrocatechol	67 BBOA	8	15.37		$C_7H_7NO_4$	168.03037 [M-H]$^-$	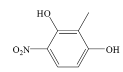 2-methyl-4-nitro-benzene-1,3-diol	37 Ambient Aerosol
4	10.35		$C_9H_{10}O_4$	181.05075 [M-H]$^-$ 183.06505 [M+H]$^+$	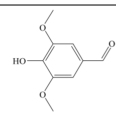 syringaldehyde	68 BBOA	9	18.35		$C_8H_9NO_5$	198.04092 [M-H]$^-$	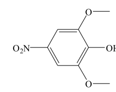 4-nitrosyringol	61 Aged BBOA
5	12.40		$C_6H_5NO_3$	138.01947 [M-H]$^-$	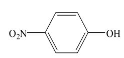 4-nitrophenol	S	10	20.48		$C_7H_7NO_4$	168.02979 [M-H]$^-$	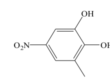 3-methyl-5-nitrocatechol	S
11	22.04		$C_7H_7NO_3$	152.03520 [M-H]$^-$	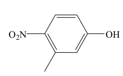 3-methyl-4-nitrophenol	S	17	37.50		$C_{10}H_7NO_3$	188.03540 [M-H]$^-$	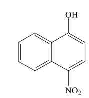 4-nitro-1-naphthol	S
12	23.86		$C_{12}H_6O_2$	183.04391 [M+H]$^+$	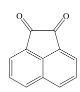 1,2-acenaphthenedione	62 Ambient aerosol	18	39.99		$C_{11}H_9NO_3$	202.05135 [M-H]$^-$	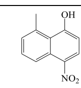 8-methyl-4-nitro-1-naphthol	37 Ambient aerosol
13	24.92		$C_{12}H_6O_3$	199.03890 [M+H]$^+$	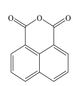 1,8-naphthalic anhydride	62 Ambient aerosol	19	43.93		$C_{15}H_8O_2$	221.05960 [M+H]$^+$	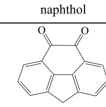 4H-Cyclopenta[def]phenanthrene-8,9-dione	57 Ambient Aerosol
14	25.62		$C_7H_7NO_3$	152.03517 [M-H]$^-$	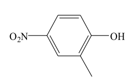 2-methyl-4-nitrophenol	S	20	47.09		$C_{17}H_{10}O$	231.08036 [M+H]$^+$	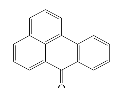 benzo[de]anthracen-7-one	57 BBOA
15	30.22		$C_8H_9NO_3$	166.05111 [M-H]$^-$	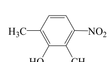 2,6-dimethyl-3-nitrophenol	37 Ambient aerosol	21	51.02		$C_{19}H_{10}O$	255.08036 [M+H]$^+$	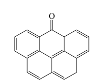 6H-benzo[cd]pyren-6-one	57 BBOA
16	34.01		$C_{13}H_8O$	181.06450 [M+H]$^+$	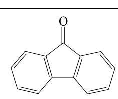 9-fluorenone	62 Ambient aerosol	22	52.05		$C_{19}H_{11}N$	254.09621 [M+H]$^+$	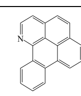 azabenzopyrene	70 Coal tar

https://dx.doi.org/10.1021/acs.est.0c01149
Environ. Sci. Technol. 2020, 54, 7836−7847

Table 2. continued

#	RT (min)	UV-Vis Spectrum	Formula	m/z & ion mech.[1]	Unambiguous/Tentative structure	Ref. Sample	#	RT (min)	UV-Vis Spectrum	Formula	m/z & ion mech.	Unambiguous/Tentative structure	Ref. Sample
23	52.35	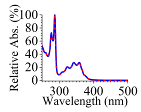	$C_{16}H_{10}$	-[3]	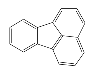 fluoranthene	S	29	57.77	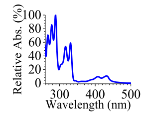	$C_{20}H_{12}$	253.10129 $[M+H]^+$	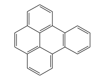 benzo(e)pyrene	62 Ambient aerosol
24	52.98	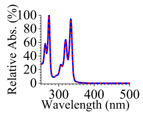	$C_{16}H_{10}$	203.08560 $[M+H]^+$	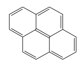 pyrene	S	30	57.85	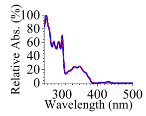	$C_{20}H_{12}$	253.10136 $[M+H]^+$	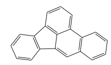 benzo(b)fluoranthene	S
25	54.95	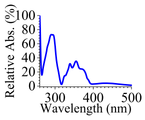	$C_{18}H_{10}$	227.08500 $[M+H]^+$	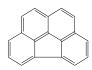 benzo[ghi]fluoranthene	54 Aged BBOA	31	58.07	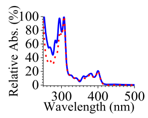	$C_{20}H_{12}$	253.10120 $[M+H]^+$	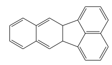 benzo(k)fluoranthene	S
26	55.40	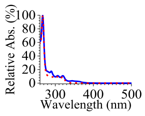	$C_{18}H_{12}$	228.09380 $[M^{\bullet}]^+$	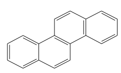 chrysene	S	32	58.45	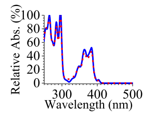	$C_{20}H_{12}$	253.10131 $[M+H]^+$	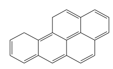 benzo(a)pyrene	S
27	55.66	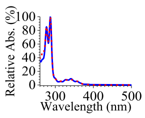	$C_{18}H_{12}$	229.10121 $[M+H]^+$	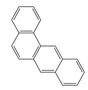 benzo(a)anthracene	S	33	60.63	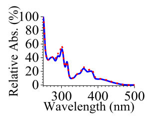	$C_{22}H_{12}$	277.10126 $[M+H]^+$	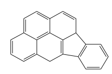 indeno(1,2,3-cd)pyrene	S
28	57.40	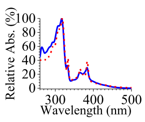	$C_{20}H_{12}$	253.10129 $[M+H]^+$	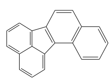 benzo(j)fluoranthene	S	34	61.53	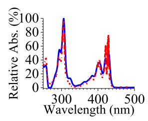	$C_{22}H_{12}$	276.09344 $[M^{\bullet}]^+$	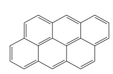 anthanthrene	71

[a]"The blue and red lines in the UV−Vis spectra represent the main chromophores in aerosol samples and the standard compounds, respectively. Legend for superscript numbers: (1) ionization mechanism $[M + H]^{\pm}$ for protonated, $[M - H]^-$ for deprotonated, and $[M^{\bullet}]^+$ for ion radical; (2) standard compounds measured in our study; (3) The MS signal was not detectable due to low ESI ionization efficiency."

spectrum and literature data, respectively. Figure S3 shows the 3D plot of HPLC-PDA absorption chromatograms of HULIS-BrC and WI-BrC, together with the assigned chemical formulas of the main BrC chromophores. A full list of the detailed information concerning the retention time, UV−vis spectrum, elemental formulas, and assigned structures of these identified BrC chromophores is summarized in Table 2. The results show that the PDA absorption profiles are very similar between Xi'an and Beijing for both HULIS-BrC and WI-BrC, and the identified chromophores are identical between Xi'an and Beijing, demonstrating that the composition of BrC chromophores between these two cities in winter may be similar to some extent despite the difference in energy for residential heating (i.e., mainly biomass burning in Xi'an and coal combustion in Beijing[60]).

Among the 18 chromophores (#1−18) identified in the HULIS-BrC fraction, 14 chromophores are identified as CHON compounds with an assigned elemental formula containing one nitrogen atom and at least three oxygen atoms. These CHON chromophores are observed only in ESI(−) mode, suggesting they might be nitrophenolic compounds (NPs). Using nitrophenol standards, seven CHON chromophores can be unambiguously assigned, including $C_6H_5NO_4$ (4-nitrocatechol, #2, RT = 7.78 min), $C_6H_5NO_3$ (4-nitrophenol, #5, RT = 12.40 min), $C_7H_7NO_4$ (4-methyl-5-nitrocatechol, #7, RT = 14.92 min; 3-methyl-5-nitrocatechol, #10, RT = 20.48 min), $C_7H_7NO_3$ (3-methyl-4-nitrophenol, #11, RT = 22.04 min; 2-methyl-4-nitrophenol, #14, RT = 25.62 min), and $C_{10}H_7NO_3$ (4-nitro-1-naphthol, #17, RT = 37.50 min) (see Table 2 and Table S1). For example, the chromophore eluted at 7.78 min with an assigned formula of $C_6H_5NO_4$ (#2) and the standard 4-nitrocatechol have the same retention times, UV−vis spectra, and mass spectra, demonstrating the presence of this NP chromophore. For the other seven CHON chromophores (#1, #3, #6, #8, #9, #15, and #18), they are tentatively assigned to nitropyrogallol (#1), 3-methoxy-4-nitrocatechol (#3), 4-nitrosalicylic acid (#6), 2-methyl-4-nitrobenzene-1,3-diol (#8), 4-nitrosyringol (#9), 2,6-dimethyl-3-nitrophenol (#15), and 8-methyl-4-nitro-1-naphthol (#18), through comparison with reference UV−vis spectra and data from previous studies.[37,61,66,67] For example, the chromophore eluted at 18.35 min with an assigned formula of $C_8H_9NO_5$ (#9) is likely 4-nitrosyringol by comparison with the reference UV−vis spectrum in the literature.[61] The other four chromophores are detected as CHO compounds, of which three (#12, #13, and #16) have a high AI value (>0.67) and a low O/C ratio (<0.1) and are detected more efficiently in ESI(+) mode, indicating that they are likely oxygenated or O-heterocyclic PAHs. Further comparison with field observations from previous studies suggests that these three CHO chromophores might be 1,2-acenaphthenedione (#12), 1,8-naphthalic anhydride (#13), and 9-fluorenone (#16), which are detected as major carbonyl-OPAH species in ambient aerosol during winter in urban Xi'an and Beijing.[62,63] Note that nitro-aromatics have been found to be abundant BrC chromophores in aged biomass burning organic aerosol and

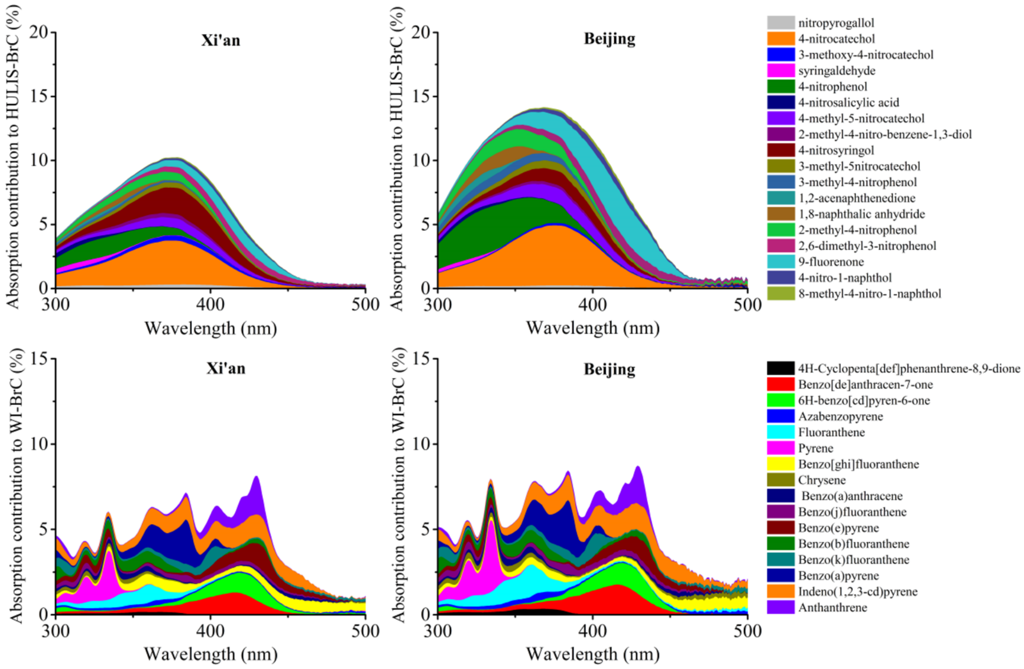

Figure 4. Relative contributions of the identified main BrC chromophores with respect to the total light absorption by BrC fractions (HULIS-BrC and WI-BrC) over the wavelength range of 300−500 nm in Xi'an and Beijing.

cloud droplets influenced by agriculture biomass-burning emissions.[39,61] Our study indicates that nitro-aromatics (mainly nitrophenols) are also abundant BrC chromophores in ambient aerosol in urban Xi'an and Beijing during the winter, which are largely influenced by emissions from residential heating.

Different from HULIS-BrC, the BrC chromophores identified in the WI-BrC fraction (#19−34, a total of 16 species) are detected in ESI(+) mode because these chromophores showed high absorption peaks in the HPLC-PDA chromatograms. Therefore, 12 chromophores (#23−34) are assigned to hydrocarbons with between 16 and 22 carbon atoms and high AI values (>0.75), indicating that they are likely unsubstituted PAHs. Using PAH standards, 9 hydrocarbon chromophores have been unambiguously assigned, including fluoranthene (#23, RT = 52.35 min), pyrene (#24, RT = 52.98 min), chrysene (#26, RT = 55.40 min), benzo[*a*]anthracene (#27, RT = 55.66 min), benzo[*j*]fluoranthene (#28, RT = 57.40 min), benzo[*b*]fluoranthene (#30, RT = 57.85 min), benzo[*k*]fluoranthene (#31, RT = 58.07 min), benzo[*a*]pyrene (#32, RT = 58.45 min) and indeno(1,2,3-cd)pyrene (#33, RT = 60.63 min) (see Table 2 and Table S1). The other three hydrocarbon chromophores are tentatively assigned as benzo[*ghi*]fluoranthene (#25), benzo[*e*]pyrene (#29), and anthanthrene (#34). Note that some isomers are well separated in this study: for example, those five isomers with a chemical formula of $C_{20}H_{12}$, i.e., benzo[*j*]fluoranthene, benzo[*b*]fluoranthene, benzo[*k*]fluoranthene, benzo[*a*]pyrene, and benzo[*e*]pyrene. In addition, three BrC chromophores (#19−21) are detected in ESI(+) mode, and each contains more than 15 carbon atoms and 1−2 oxygens with AI > 0.76, suggesting they are likely oxygenated or O-heterocyclic PAHs. Further comparison with the BrC chromophores identified in biomass-burning organic aerosol indicates that these three chromophores could be 4*H*-cyclopenta[*def*]phenanthrene-8,9-dione (#19), benzo[*de*]anthracen-7-one (#20), and 6*H*-benzo[*cd*]pyren-6-one (#21).[57] In addition, we observed one OPAH chromophore with a chemical formula of $C_{14}H_8O_2$ (m/z 209.0594) at RT = 41.98 min, which is likely 9,10-anthraquinone, one of the most abundant OPAHs in $PM_{2.5}$ samples collected in Xi'an and Beijing during the wintertime.[62,69] However, due to its low absorbance abundance, it is not included in the identified main BrC chromophore list. Although there have been many studies associated with the chemical composition, sources, and toxic effects of atmospheric PAHs and their derivatives,[63−65] few have investigated their contribution to and effect on the light absorption of BrC in atmospheric aerosol.[54] Our results suggest that PAHs and their derivatives are also an important class of BrC chromophores of ambient aerosol.

The contributions of these identified HULIS-BrC and WI-BrC chromophores to the overall light absorption were evaluated by comparing the light absorptions of individual chromophores with those of the corresponding BrC fractions measured by direct injection without column separation, and the results are shown in Figure 4. It can be seen that the absorption of these chromophores is wavelength dependent between 300 and 500 nm. Specifically, the chromophores identified in HULIS-BrC show only one peak and their contributions to the light absorption of the HULIS-BrC fraction increase from 4% and 6% at 300 nm to 10% and 14% at 370 nm and then decrease to below 1% at 500 nm in Xi'an and Beijing, respectively. On average, these chromophores contribute 5% and 8% of the light absorption of HULIS-BrC fraction in the wavelength range of 300−500 nm in Xi'an and Beijing, respectively. The main contributors are 4-nitrocatechol, 4-nitrophenol, 4-nitrosyringol, and 9-fluorenone, which account for a total of ∼60% of the light absorption of these identified BrC chromophores in HULIS-BrC over the wavelength range of 300−500 nm. However, the chromophores in WI-BrC show multiple peaks and large differences in light absorption contributions at different wavelength, which could be attributed to the large difference in absorption spectra of PAHs and their derivatives (see Table 2). For example, the

https://dx.doi.org/10.1021/acs.est.0c01149
Environ. Sci. Technol. 2020, 54, 7836−7847

contributions of pyrene to the light absorption of WI-BrC fraction are 3% and 4% at 334 nm and decreases to negligible at 384 nm in Xi'an and Beijing, respectively, while the contributions of benzo[*a*]pyrene to the light absorption of WI-BrC fraction are 2.6% and 2.9% at 384 nm and are negligible at 334 nm in Xi'an and Beijing, respectively. In general, the contribution above 400 nm is mainly related to benzo[*de*]-anthracen-7-one, 6H-benzo[*cd*]pyren-6-one, benzo[*e*]pyrene, anthanthrene, and indeno[1,2,3-*cd*]pyrene, and the contribution between 350 and 400 nm is mainly from fluoranthene, benzo[ghi]fluoranthene, benzo[*b*]fluoranthene, benzo[*a*]-pyrene and indeno[1,2,3-*cd*]pyrene, while the contribution below 350 nm is mainly from fluoranthene, pyrene and benzo[*b*]fluoranthene. On average, the light absorption contributions of these identified chromophores to the light absorption of the WI-BrC fraction are 4% and 5% over the wavelength range of 300−500 nm in Xi'an and Beijing, respectively. It is possible that PAHs with high molecular weights may not be fully extracted by methanol. Therefore, our result provides a lower limit estimate of their light absorption contributions.

Although 18 chromophores in HULIS-BrC and 16 chromophores in WI-BrC in urban atmospheric aerosol are identified in our study, including those newly identified chromophores such as 4-nitrosyringol, 1,2-acenaphthenedione, 1,8-naphthalic anhydride, 9-fluorenone, benzo[*de*]anthracen-7-one, 6H-benzo[*cd*]pyren-6-one, and anthanthrene, these BrC species only explain a small fraction of BrC light absorption (10% and 14% for HULIS-BrC and 6% and 8% for WI-BrC at 365 nm in Xi'an and Beijing, respectively). This suggests that both HULIS-BrC and WI-BrC likely consist of a number of chromophores and each has a small contribution to the absorption. The low concentrations and complex mixtures make the separation and identification of BrC chromophores a very challenging task. In particular, since water-insoluble fraction dominate BrC (51 ± 5% and 62 ± 13% in Xi'an and Beijing, respectively), more studies are needed to characterize the chemical composition and the link with light absorption properties for the WI-BrC fraction. The low ESI ionization efficiency for nonpolar organic molecules, however, hinders the identification of those WI-BrC chromophores with low concentrations. Future studies should combine 2D HPLC-PDA-HRMS with different ionization techniques (e.g., atmospheric-pressure photoionization[54]) to provide a more comprehensive characterization of BrC chromophores in ambient aerosol."

■ ASSOCIATED CONTENT

Supporting Information

The Supporting Information is available free of charge at https://pubs.acs.org/doi/10.1021/acs.est.0c01149.

> HPLC retention times of the nitrophenols and PAH standard compounds, solvent extraction procedure of different OC and BrC fractions, light absorption spectra of different BrC fractions, 3D-plot of HPLC/PDA chromatograms of BrC fractions (PDF)

■ AUTHOR INFORMATION

Corresponding Authors

Ru-Jin Huang − *State Key Laboratory of Loess and Quaternary Geology, Center for Excellence in Quaternary Science and Global Change, and Key Laboratory of Aerosol Chemistry and Physics, Institute of Earth Environment, Chinese Academy of Sciences, Xi'an 710061, People's Republic of China; Institute of Global Environmental Change, Xi'an Jiaotong University, Xi'an 710049, People's Republic of China; Open Studio for Oceanic-Continental Climate and Environment Changes, Pilot National Laboratory for Marine Science and Technology (Qingdao), Qingdao 266061, People's Republic of China;* orcid.org/0000-0002-4907-9616; Email: rujin.huang@ieecas.cn

Jincan Shen − *Key Laboratory of Detection Technology R & D on Food Safety, Food Inspection and Quarantine Technology Center of Shenzhen Customs, Shenzhen 518045, People's Republic of China*; Email: jincansh@263.net

Authors

Lu Yang − *State Key Laboratory of Loess and Quaternary Geology, Center for Excellence in Quaternary Science and Global Change, and Key Laboratory of Aerosol Chemistry and Physics, Institute of Earth Environment, Chinese Academy of Sciences, Xi'an 710061, People's Republic of China*

Wei Yuan − *State Key Laboratory of Loess and Quaternary Geology, Center for Excellence in Quaternary Science and Global Change, and Key Laboratory of Aerosol Chemistry and Physics, Institute of Earth Environment, Chinese Academy of Sciences, Xi'an 710061, People's Republic of China*

Yuquan Gong − *State Key Laboratory of Loess and Quaternary Geology, Center for Excellence in Quaternary Science and Global Change, and Key Laboratory of Aerosol Chemistry and Physics, Institute of Earth Environment, Chinese Academy of Sciences, Xi'an 710061, People's Republic of China*

Jie Guo − *State Key Laboratory of Loess and Quaternary Geology, Center for Excellence in Quaternary Science and Global Change, and Key Laboratory of Aerosol Chemistry and Physics, Institute of Earth Environment, Chinese Academy of Sciences, Xi'an 710061, People's Republic of China*

Wenjuan Cao − *State Key Laboratory of Loess and Quaternary Geology, Center for Excellence in Quaternary Science and Global Change, and Key Laboratory of Aerosol Chemistry and Physics, Institute of Earth Environment, Chinese Academy of Sciences, Xi'an 710061, People's Republic of China*

Jing Duan − *State Key Laboratory of Loess and Quaternary Geology, Center for Excellence in Quaternary Science and Global Change, and Key Laboratory of Aerosol Chemistry and Physics, Institute of Earth Environment, Chinese Academy of Sciences, Xi'an 710061, People's Republic of China*

Haiyan Ni − *State Key Laboratory of Loess and Quaternary Geology, Center for Excellence in Quaternary Science and Global Change, and Key Laboratory of Aerosol Chemistry and Physics, Institute of Earth Environment, Chinese Academy of Sciences, Xi'an 710061, People's Republic of China; Centre for Isotope Research (CIO), Energy and Sustainability Research Institute Groningen (ESRIG), University of Groningen, 9747 AG Groningen, The Netherlands*

Chongshu Zhu − *State Key Laboratory of Loess and Quaternary Geology, Center for Excellence in Quaternary Science and Global Change, and Key Laboratory of Aerosol Chemistry and Physics, Institute of Earth Environment, Chinese Academy of Sciences, Xi'an 710061, People's Republic of China*

Wenting Dai − *State Key Laboratory of Loess and Quaternary Geology, Center for Excellence in Quaternary Science and Global Change, and Key Laboratory of Aerosol Chemistry and Physics, Institute of Earth Environment, Chinese Academy of Sciences, Xi'an 710061, People's Republic of China*

https://dx.doi.org/10.1021/acs.est.0c01149
Environ. Sci. Technol. 2020, 54, 7836−7847

Yongjie Li − *Department of Civil and Environmental Engineering, Faculty of Science and Technology, University of Macau, Taipa, Macau 999078, People's Republic of China*
Yang Chen − *Chongqing Institute of Green and Intelligent Technology, Chinese Academy of Sciences, Chongqing 400714, People's Republic of China*
Qi Chen − *State Key Joint Laboratory of Environmental Simulation and Pollution Control, College of Environmental Sciences and Engineering, Peking University, Beijing 100871, People's Republic of China*
Yunfei Wu − *RCE-TEA, Institute of Atmospheric Physics, Chinese Academy of Sciences, Beijing 100029, People's Republic of China*
Renjian Zhang − *RCE-TEA, Institute of Atmospheric Physics, Chinese Academy of Sciences, Beijing 100029, People's Republic of China*
Ulrike Dusek − *Centre for Isotope Research (CIO), Energy and Sustainability Research Institute Groningen (ESRIG), University of Groningen, 9747 AG Groningen, The Netherlands*
Colin O'Dowd − *School of Physics and Centre for Climate and Air Pollution Studies, Ryan Institute, National University of Ireland Galway, Galway H91CF50, Ireland*
Thorsten Hoffmann − *Institute of Inorganic and Analytical Chemistry, Johannes Gutenberg University of Mainz, Mainz 55128, Germany*

Complete contact information is available at:
https://pubs.acs.org/10.1021/acs.est.0c01149

Notes

The authors declare no competing financial interest.

■ ACKNOWLEDGMENTS

This work was supported by the National Natural Science Foundation of China (NSFC) under Grant Nos. 41877408, 41925015, 91644219, and 41675120, the Chinese Academy of Sciences (No. ZDBS-LY-DQC001), the National Key Research and Development Program of China (No. 2017YFC0212701), and the Cross Innovative Team fund from the State Key Laboratory of Loess and Quaternary Geology (No. SKLLQGTD1801).

■ REFERENCES

(1) Andreae, M. O.; Gelencser, A. Black carbon or brown carbon? The nature of light-absorbing carbonaceous aerosols. *Atmos. Chem. Phys.* **2006**, *6*, 3131−3148.
(2) Alexander, D. T. L.; Crozier, P. A.; Anderson, J. R. Brown carbon spheres in East Asian outflow and their optical properties. *Science* **2008**, *321*, 833−836.
(3) Doherty, S. J.; Warren, S. G.; Grenfell, T. C.; Clarke, A. D.; Brandt, R. E. Light absorbing impurities in Arctic snow. *Atmos. Chem. Phys.* **2010**, *10*, 11647−11680.
(4) Lack, D. A.; Cappa, C. D. Impact of brown and clear carbon on light absorption enhancement, single scatter albedo and absorption wavelength dependence of black carbon. *Atmos. Chem. Phys.* **2010**, *10*, 4207−4220.
(5) Bahadur, R.; Praveen, P. S.; Xu, Y.; Ramanathan, V. Solar absorption by elemental and brown carbon determined from spectral observations. *Proc. Natl. Acad. Sci. U. S. A.* **2012**, *109*, 17366−17371.
(6) Kirillova, E. N.; Marinoni, A.; Bonasoni, P.; Vuillermoz, E.; Facchini, M. C.; Fuzzi, S.; Decesari, S. Light absorption properties of brown carbon in the high Himalayas. *J. Geophys. Res. Atmos.* **2016**, *121*, 9621−9639.
(7) Washenfelder, R. A.; Attwood, A. R.; Brock, C. A.; Guo, H.; Xu, L.; Weber, R. J.; Ng, N. L.; Allen, H. M.; Ayres, B. R.; Baumann, K.; Cohen, R. C.; Draper, D. C.; Duffey, K. C.; Edgerton, E.; Fry, J. L.; Hu, W.; Jimenez, J. L.; Palm, B. B.; Romer, P.; Stone, E. A.; Wooldridge, P. J.; Brown, S. S. Biomass burning dominates brown carbon absorption in the rural southeastern United States. *Geophys. Res. Lett.* **2015**, *42*, 653−664.
(8) Costabile, F.; Gilardoni, S.; Barnaba, F.; Di Ianni, A.; Di Liberto, L.; Dionisi, D.; Manigrasso, M.; Paglione, M.; Poluzzi, V.; Rinaldi, M.; Facchini, M. C.; Gobbi, G. P. Characteristics of brown carbon in the urban Po Valley atmosphere. *Atmos. Chem. Phys.* **2017**, *17*, 313−326.
(9) Jacobson, M. Z. Studying the effects of aerosols on vertical photolysis rate coefficient and temperature profiles over an urban airshed. *J. Geophys. Res.* **1998**, *103*, 10593.
(10) Feng, Y.; Ramanathan, V.; Kotamarthi, V. R. Brown carbon: A significant atmospheric absorber of solar radiation? *Atmos. Chem. Phys.* **2013**, *13*, 8607−8621.
(11) Hammer, M. S.; Martin, R. V.; van Donkelaar, A.; Buchard, V.; Torres, O.; Ridley, D. A.; Spurr, R. J. D. Interpreting the ultraviolet aerosol index observed with the OMI satellite instrument to understand absorption by organic aerosols: Implications for atmospheric oxidation and direct radiative effects. *Atmos. Chem. Phys.* **2016**, *16*, 2507−2523.
(12) Mok, J.; Krotkov, N.; Arola, A.; Torres, O.; Jethva, H.; Andrade, M.; Labow, G.; Eck, T. F.; Li, Z. Q.; Dickerson, R. R.; Stenchikov, G. L.; Osipov, S.; Ren, X. R. Impacts of brown carbon from biomass burning on surface UV and ozone photochemistry in the Amazon Basin. *Sci. Rep.* **2016**, *6*, 36940.
(13) Zhang, Y.; Forrister, H.; Liu, J.; Dibb, J.; Anderson, B.; Schwarz, J. P.; Perring, A. E.; Jimenez, J. L.; Campuzano-Jost, P.; Wang, Y.; Nenes, A.; Weber, R. J. Top-of-atmosphere radiative forcing affected by brown carbon in the upper troposphere. *Nat. Geosci.* **2017**, *10*, 486−489.
(14) Brown, H.; Liu, X.; Feng, Y.; Jiang, Y.; Wu, M.; Lu, Z.; Wu, C.; Murphy, S.; Pokhrel, R. Radiative effect and climate impacts of brown carbon with the Community Atmosphere Model (CAM5). *Atmos. Chem. Phys.* **2018**, *18*, 17745−17768.
(15) Chen, Y.; Bond, T. C. Light absorption by organic carbon from wood combustion. *Atmos. Chem. Phys.* **2010**, *10*, 1773−1787.
(16) Hecobian, A.; Zhang, X.; Zheng, M.; Frank, N. H.; Edgerton, E. S.; Weber, R. J. Water-soluble organic aerosol material and the light absorption characteristics of aqueous extracts measured over the Southeastern United States. *Atmos. Chem. Phys.* **2010**, *10*, 5965−5977.
(17) Saleh, R.; Robinson, E. S.; Tkacik, D. S.; Ahern, A. T.; Liu, S.; Aiken, A. C.; Sullivan, R. C.; Presto, A. A.; Dubey, M. K.; Yokelson, R. J.; Donahue, N. M.; Robinson, A. L. Brownness of organics in aerosols from biomass burning linked to their black carbon content. *Nat. Geosci.* **2014**, *7*, 647−650.
(18) Du, Z. Y.; He, K. B.; Cheng, Y.; Duan, F. K.; Ma, Y. L.; Liu, J. M.; Zhang, X. L.; Zheng, M.; Weber, R. J. A yearlong study of water-soluble organic carbon in Beijing II: Light absorption properties. *Atmos. Environ.* **2014**, *89*, 235−241.
(19) Yan, C.; Zheng, M.; Sullivan, A. P.; Bosch, C.; Desyaterik, Y.; Andersson, A.; Li, X.; Guo, X.; Zhou, T.; Gustafsson, Ö.; Collett, J. L., Jr Chemical characteristics and light absorbing property of water-soluble organic carbon in Beijing: Biomass burning contributions. *Atmos. Environ.* **2015**, *121*, 4−12.
(20) Liu, J.; Scheuer, E.; Dibb, J.; Diskin, G. S.; Ziemba, L. D.; Thornhill, K. L.; Anderson, B. E.; Wisthaler, A.; Mikoviny, T.; Devi, J. J.; Bergin, M.; Perring, A. E.; Markovic, M. Z.; Schwarz, J. P.; Campuzano-Jost, P.; Day, D. A.; Jimenez, J. L.; Weber, R. J. Brown carbon aerosol in the North American continental troposphere: Sources, abundance, and radiative forcing. *Atmos. Chem. Phys.* **2015**, *15*, 7841−7858.
(21) Ma, Y.; Cheng, Y.; Qiu, X.; Cao, G.; Kuang, B.; Yu, J. Z.; Hu, D. Optical properties, source apportionment and redox activity of humic-like substances (HULIS) in airborne fine particulates in Hong Kong. *Environ. Pollut.* **2019**, *255* (1), 113087.
(22) Cheng, Y.; He, K. B.; Engling, G.; Weber, R.; Liu, J. M.; Du, Z. Y.; Dong, S. P. Brown and black carbon in Beijing aerosol:

Implications for the effects of brown coating on light absorption by black carbon. *Sci. Total Environ.* **2017**, *599–600*, 1047−1055.
(23) Chen, T. F.; Ge, X. L.; Chen, H.; Xie, X. C.; Chen, Y. T.; Wang, J. F.; Ye, Z. L.; Bao, M. Y.; Zhang, Y. L.; Chen, M. D. Seasonal light absorption properties of water-soluble brown carbon in atmospheric fine particles in Nanjing. *Atmos. Environ.* **2018**, *187*, 230−240.
(24) Wu, G. M.; Wan, X.; Gao, S. P.; Fu, P. Q.; Yin, Y. G.; Li, G.; Zhang, G. S.; Kang, S. C.; Ram, K.; Cong, Z. Y. Humic-Like Substances (HULIS) in aerosols of central Tibetan Plateau (Nam Co, 4730 m asl): Abundance, light absorption properties, and sources. *Environ. Sci. Technol.* **2018**, *52*, 7203−7211.
(25) Ma, Y.; Cheng, Y.; Qiu, X.; Cao, G.; Fang, Y.; Wang, J.; Zhu, T.; Yu, J. Z.; Hu, D. Sources and oxidative potential of water-soluble humic like substances ($HULIS_{WS}$) in fine particulate matter ($PM_{2.5}$) in Beijing. *Atmos. Chem. Phys.* **2018**, *18*, 5607−5617.
(26) Xie, M. J.; Chen, X.; Holder, A. L.; Hays, M. D.; Lewandowski, M.; Offenberg, J. H.; Kleindienst, T. E.; Jaoui, M.; Hannigan, M. P. Light absorption of organic carbon and its sources at a southeastern U.S. location in summer. *Environ. Pollut.* **2019**, *244*, 38−46.
(27) Kirchstetter, T. W.; Novakov, T.; Hobbs, P. V. Evidence that the spectral dependence of light absorption by aerosols is affected by organic carbon. *J. Geophys. Res.-Atmos.* **2004**, *109*, D21208.
(28) Saleh, R.; Hennigan, C. J.; McMeeking, G. R.; Chuang, W. K.; Robinson, E. S.; Coe, H.; Donahue, N. M.; Robinson, A. L. Absorptivity of brown carbon in fresh and photo-chemically aged biomass-burning emissions. *Atmos. Chem. Phys.* **2013**, *13*, 7683−7693.
(29) Sun, J. Z.; Zhi, G. R.; Hitzenberger, R.; Chen, Y. J.; Tian, C. G.; Zhang, Y. Y.; Feng, Y. L.; Cheng, M. M.; Zhang, Y. Z.; Cai, J.; Chen, F.; Qiu, Y.; Jiang, Z.; Li, J.; Zhang, G.; Mo, Y. Emission factors and light absorption properties of brown carbon from household coal combustion in China. *Atmos. Chem. Phys.* **2017**, *17*, 4769−4780.
(30) Li, M. J.; Fan, X. J.; Zhu, M. B.; Zou, C. L.; Song, J. Z.; Wei, S. Y.; Jia, W. L.; Peng, P. A. Abundance and light absorption properties of brown carbon emitted from residential coal combustion in China. *Environ. Sci. Technol.* **2019**, *53*, 595−603.
(31) Powelson, M. H.; Espelien, B. M.; Hawkins, L. N.; Galloway, M. M.; Haan, D. O. D. Brown carbon formation by aqueous phase carbonyl compound reactions with amines and ammonium sulfate. *Environ. Sci. Technol.* **2014**, *48*, 985−993.
(32) De Haan, D. O.; Hawkins, L. N.; Welsh, H. G.; Pednekar, R.; Casar, J. R.; Pennington, E. A.; de Loera, A.; Jimenez, N. G.; Symons, M. A.; Zauscher, M.; Pajunoja, A.; Caponi, L.; Cazaunau, M.; Formenti, P.; Gratien, A.; Pangui, E.; Doussin, J. F. Brown carbon production in ammonium- or amine-containing aerosol particles by reactive uptake of methylglyoxal and photolytic cloud cycling. *Environ. Sci. Technol.* **2017**, *51*, 7458−7466.
(33) Liu, J. M.; Lin, P.; Laskin, A.; Laskin, J.; Kathmann, S. M.; Wise, M.; Caylor, R.; Imholt, F.; Selimovic, V.; Shilling, J. E. Optical properties and aging of light-absorbing secondary organic aerosol. *Atmos. Chem. Phys.* **2016**, *16*, 12815−12827.
(34) Lee, H. J.; Aiona, P. K.; Laskin, A.; Laskin, J.; Nizkorodov, S. A. Effect of solar radiation on the optical properties and molecular composition of laboratory proxies of atmospheric brown carbon. *Environ. Sci. Technol.* **2014**, *48*, 10217−10226.
(35) Zhong, M.; Jang, M. Dynamic light absorption of biomass burning organic carbon photochemically aged under natural sunlight. *Atmos. Chem. Phys.* **2014**, *14*, 1517−1525.
(36) Laskin, J.; Laskin, A.; Nizkorodov, S. A.; Roach, P.; Eckert, P.; Gilles, M. K.; Wang, B. B.; Lee, H. J.; Hu, Q. C. Molecular selectivity of brown carbon chromophores. *Environ. Sci. Technol.* **2014**, *48*, 12047−12055.
(37) Zhang, X. L.; Lin, Y. H.; Surratt, J. D.; Weber, R. J. Sources, composition and absorption Ångström exponent of light-absorbing organic components in aerosol extracts from the Los Angeles Basin. *Environ. Sci. Technol.* **2013**, *47*, 3685−3693.
(38) Mohr, C.; Lopez-Hilfiker, F. D.; Zotter, P.; Prévôt, A. S.; Xu, L.; Ng, N. L.; Herndon, S. C.; Williams, L. R.; Franklin, J. P.; Zahniser, M. S.; Worsnop, D. R.; Knighton, W. B.; Aiken, A. C.; Gorkowski, K. J.; Dubey, M. K.; Allan, J. D.; Thornton, J. A. Contribution of nitrated phenols to wood burning brown carbon light absorption in Detling, UK during winter time. *Environ. Sci. Technol.* **2013**, *47*, 6316−6324.
(39) Desyaterik, Y.; Sun, Y.; Shen, X.; Lee, T.; Wang, X.; Wang, T.; Collett, J. L. Speciation of brown carbon in cloud water impacted by agricultural biomass burning in eastern China. *J. Geophys. Res.- Atmos.* **2013**, *118*, 7389−7399.
(40) Huang, R. J.; Yang, L.; Cao, J. J.; Chen, Y.; Chen, Q.; Li, Y. J.; Duan, J.; Zhu, C. C.; Dai, W. T.; Wang, K.; Lin, C. S.; Ni, H. Y.; Corbin, J. C.; Wu, Y. F.; Zhang, R. J.; Tie, X. X.; Hoffmann, T.; O'Dowd, C.; Dusek, U. Brown carbon aerosol in urban Xi'an, Northwest China: The composition and light absorption properties. *Environ. Sci. Technol.* **2018**, *52*, 6825−6833.
(41) Laskin, A.; Laskin, J.; Nizkorodov, S. A. Chemistry of atmospheric brown carbon. *Chem. Rev.* **2015**, *115*, 4335−4382.
(42) Liu, J.; Bergin, M.; Guo, H.; King, L.; Kotra, N.; Edgerton, E.; Weber, R. J. Size-resolved measurements of brown carbon in water and methanol extracts and estimates of their contribution to ambient fine-particle light absorption. *Atmos. Chem. Phys.* **2013**, *13*, 12389−12404.
(43) Liu, J.; Scheuer, E.; Dibb, J.; Ziemba, L. D.; Thornhill, K. L.; Anderson, B. E.; Wisthaler, A.; Mikoviny, T.; Devi, J. J.; Bergin, M. Brown carbon in the continental troposphere. *Geophys. Res. Lett.* **2014**, *41*, 2191.
(44) Cheng, Y.; He, K. B.; Du, Z. Y.; Engling, G.; Liu, J. M.; Ma, Y. L.; Zheng, M.; Weber, R. J. The characteristics of brown carbon aerosol during winter in Beijing. *Atmos. Environ.* **2016**, *127*, 355−364.
(45) Chen, Q.; Ikemori, F.; Mochida, M. Light Absorption and Excitation−Emission Fluorescence of Urban Organic Aerosol Components and Their Relationship to Chemical Structure. *Environ. Sci. Technol.* **2016**, *50* (20), 10859−10868.
(46) Chen, Q.; Ikemori, F.; Higo, H.; Asakawa, D.; Mochida, M. Insight Into Chemical Characteristics of Aerosol HULIS and Other Fractionated Complex Matters Using Mass Spectrometry and FT-IR Spectroscopy. *Environ. Sci. Technol.* **2016**, *50* (4), 1721−1730.
(47) Kim, H.; Kim, J. Y.; Jin, H. C.; Lee, J. Y.; Lee, S. P. Seasonal variations in the light-absorbing properties of water-soluble and insoluble organic aerosols in Seoul, Korea. *Atmos. Environ.* **2016**, *129*, 234−242.
(48) Yan, F. P.; Kang, S. C.; Sillanpää, M.; Hu, Z. F.; Gao, S. P.; Chen, P. F.; Gautam, S.; Reinikainen, S.; Li, C. L. A new method for extraction of methanol-soluble brown carbon: Implications for investigation of its light absorption ability. *Environ. Pollut.* **2020**, *262*, 114300.
(49) Varga, B.; Kiss, G.; Ganszky, I.; Gelencsér, A.; Krivácsy, Z. Isolation of water soluble organic matter from atmospheric aerosol. *Talanta* **2001**, *55*, 561−572.
(50) Lin, P.; Huang, X. F.; He, L. Y.; Yu, J. Z. Abundance and size distribution of HULIS in ambient aerosols at a rural site in south China. *J. Aerosol Sci.* **2010**, *41*, 74−87.
(51) Chow, J. C.; Watson, J. G.; Robles, J.; Wang, X. L.; Chen, L. W. A.; Trimble, D. L.; Kohl, S. D.; Tropp, R. J.; Fung, K. K. Quality assurance and quality control for thermal/optical analysis of aerosol samples for organic and elemental carbon. *Anal. Bioanal. Chem.* **2011**, *401*, 3141−3152.
(52) Ho, K. F.; Ho, S. S. H.; Huang, R. J.; Liu, S. X.; Cao, J. J.; Zhang, T.; Chuang, H. C.; Chan, C. S.; Hu, D.; Tian, L. Characteristics of water-soluble organic nitrogen in fine particulate matter in the continental area of China. *Atmos. Environ.* **2015**, *106*, 252−261.
(53) Lin, P.; Rincon, A. G.; Kalberer, M.; Yu, J. Z. Elemental Composition of HULIS in the Pearl River Delta Region, China: Results Inferred from Positive and Negative Electrospray High Resolution Mass Spectrometric Data. *Environ. Sci. Technol.* **2012**, *46*, 7454−7462.
(54) Lin, P.; Fleming, L. T.; Nizkorodov, S. A.; Laskin, J.; Laskin, A. Comprehensive molecular characterization of atmospheric brown carbon by high resolution mass spectrometry with electrospray and atmospheric pressure photoionization. *Anal. Chem.* **2018**, *90*, 12493−12502.

https://dx.doi.org/10.1021/acs.est.0c01149
Environ. Sci. Technol. 2020, 54, 7836−7847

(55) Koch, B. P.; Dittmar, T. From mass to structure: an aromaticity index for high-resolution mass data of natural organic matter. *Rapid Commun. Mass Spectrom.* **2006**, *20* (5), 926−932.
(56) Phillips, S. M.; Smith, G. D. Light absorption by charge transfer complexes in brown carbon aerosols. *Environ. Sci. Technol. Lett.* **2014**, *1*, 382−386.
(57) Lin, P.; Aiona, P. K.; Li, Y.; Shiraiwa, M.; Laskin, J.; Nizkorodov, S. A.; Laskin, A. Molecular characterization of Brown carbon in biomass burning aerosol particles. *Environ. Sci. Technol.* **2016**, *50*, 11815−11824.
(58) Lin, P.; Liu, J. M.; Shilling, J. E.; Kathmann, S. M.; Laskin, J.; Laskin, A. Molecular characterization of brown carbon (BrC) chromophores in secondary organic aerosol generated from photo-oxidation of toluene. *Phys. Chem. Chem. Phys.* **2015**, *17*, 23312−23325.
(59) Budisulistiorini, S. H.; Riva, M.; Williams, M.; Chen, J.; Itoh, M.; Surratt, J. D.; Kuwata, M. Light-absorbing brown carbon aerosol constituents from combustion of indonesian peat and biomass. *Environ. Sci. Technol.* **2017**, *51*, 4415−4423.
(60) Elser, M.; Huang, R.-J.; Wolf, R.; Slowik, J. G.; Wang, Q.; Canonaco, F.; Li, G.; Bozzetti, C.; Daellenbach, K. R.; Huang, Y.; Zhang, R.; Li, Z.; Cao, J.; Baltensperger, U.; El-Haddad, I.; Prévôt, A. S. H. New insights into $PM_{2.5}$ chemical composition and sources in two major cities in China during extreme haze events using aerosol mass spectrometry. *Atmos. Chem. Phys.* **2016**, *16*, 3207−3225.
(61) Lin, P.; Bluvshtein, N.; Rudich, Y.; Nizkorodov, S.; Laskin, J.; Laskin, A. Molecular chemistry of atmospheric brown carbon inferred from a nationwide biomass burning event. *Environ. Sci. Technol.* **2017**, *51*, 11561−11570.
(62) Bandowe, B. A. M.; Meusel, H.; Huang, R. J.; Ho, K. F.; Cao, J. J.; Hoffmann, T.; Wilcke, W. $PM_{2.5}$-bound oxygenated PAHs, nitro-PAHs and parent-PAHs from the atmosphere of a Chinese megacity: Seasonal variation, sources and cancer risk assessment. *Sci. Total Environ.* **2014**, *473*, 77−87.
(63) Niu, X. Y.; Ho, S. S. H.; Ho, K. F.; Huang, Y.; Sun, J.; Wang, Q. Y.; Zhou, Y. Q.; Zhao, Z. Z.; Cao, J. J. Atmospheric levels and cytotoxicity of polycyclic aromatic hydrocarbons and oxygenated-PAHs in $PM_{2.5}$ in the Beijing-Tianjin-Hebei region. *Environ. Pollut.* **2017**, *231*, 1075−1084.
(64) Kim, K.-H.; Jahan, S. A.; Kabir, E.; Brown, R. J. C. A review of airborne polycyclic aromatic hydrocarbons (PAHs) and their human health effects. *Environ. Int.* **2013**, *60*, 71−80.
(65) Zhang, Y.; Lin, Y.; Cai, J.; Liu, Y.; Hong, L.; Qin, M. M.; Zhao, Y. F.; Ma, J.; Wang, X. S.; Zhu, T.; Qiu, X. H.; Zheng, M. Atmospheric PAHs in North China: Spatial distribution and sources. *Sci. Total Environ.* **2016**, *565*, 994−1000.
(66) Fleming, L. T.; Lin, P.; Roberts, J. M.; Selimovic, V.; Yokelson, R.; Laskin, J.; Laskin, A.; Nizkorodov, S. A. Molecular composition and photochemical lifetimes of brown carbon chromophores in biomass burning organic aerosol. *Atmos. Chem. Phys.* **2020**, *20*, 1105−1129.
(67) Xie, M.; Chen, X.; Hays, M. D.; Holder, A. L. Composition and light absorption of N-containing aromatic compounds in organic aerosols from laboratory biomass burning. *Atmos. Chem. Phys.* **2019**, *19*, 2899−2915.
(68) Oros, D. R.; bin Abas, M. R.; Omar, N. Y. M. J.; Rahman, N. A.; Simoneit, B. R. T. Identification and emission factors of molecular tracers in organic aerosols from biomass burning Part 3. Grasses. *Appl. Geochem.* **2006**, *21*, 919−940.
(69) Lin, Y.; Ma, Y.; Qiu, X.; Li, R.; Fang, Y.; Wang, J.; Zhu, Y.; Hu, D. Sources, transformation, and health implications of polycyclic aromatic hydrocarbons (PAHs) and their nitrated, hydroxylated, and oxygenated derivatives in fine particulate matter ($PM_{2.5}$) in Beijing. *J. Geophys. Res.-Atmos.* **2015**, *120*, 7219−7228.
(70) Herod, A. A.; Millan, M.; Morgan, T.; Li, W. Y.; Feng, J.; Kandiyoti, R. Positive-ion electrospray ionisation mass spectrometry of acetone- and acetonitrile-soluble fractions of coal-derived liquids. *Eur. J. Mass Spectrom.* **2005**, *11*, 429−442.
(71) Johannessen, C.; Gorski, A.; Waluk, J.; Spanget-Larsen, J. Electronic states of anthanthrene. Linear and magnetic circular dichroism, fluorescence anisotropy, and quantum chemical calculations. *Polycyclic Aromat. Compd.* **2005**, *25*, 23−45.

https://dx.doi.org/10.1021/acs.est.0c01149
Environ. Sci. Technol. 2020, 54, 7836−7847